Journal of Experimental Botany, Vol. 62, No. 11, pp. 3929–3939, 2011
doi:10.1093/jxb/err090 Advance Access publication 29 March, 2011
This paper is available online free of all access charges (see http://jxb.oxfordjournals.org/open_access.html for further details)

Journal of Experimental Botany
www.jxb.oxfordjournals.org

RESEARCH PAPER

New insights into globoids of protein storage vacuoles in wheat aleurone using synchrotron soft X-ray microscopy

Marjana Regvar[1], Diane Eichert[2], Burkhard Kaulich[2], Alessandra Gianoncelli[2], Paula Pongrac[1,3], Katarina Vogel-Mikuš[1] and Ivan Kreft[1,*]

[1] Biotechnical Faculty, University of Ljubljana, Jamnikarjeva 101, SI-1000 Ljubljana, Slovenia
[2] Sincrotrone Trieste, S.S. 14, km 163.5 in Area Science Park, I-34149 Trieste, Italy
[3] Jožef Stefan Institute, Jamova 39, SI-1000 Ljubljana, Slovenia

* To whom correspondence should be addressed. E-mail: ivan.kreft@guest.arnes.si

Received 15 January 2011; Revised 3 March 2011; Accepted 4 March 2011

Abstract

Mature developed seeds are physiologically and biochemically committed to store nutrients, principally as starch, protein, oils, and minerals. The composition and distribution of elements inside the aleurone cell layer reflect their biogenesis, structural characteristics, and physiological functions. It is therefore of primary importance to understand the mechanisms underlying metal ion accumulation, distribution, storage, and bioavailability in aleurone subcellular organelles for seed fortification purposes. Synchrotron radiation soft X-ray full-field imaging mode (FFIM) and low-energy X-ray fluorescence (LEXRF) spectromicroscopy were applied to characterize major structural features and the subcellular distribution of physiologically important elements (Zn, Fe, Na, Mg, Al, Si, and P). These direct imaging methods reveal the accumulation patterns between the apoplast and symplast, and highlight the importance of globoids with phytic acid mineral salts and walls as preferential storage structures. C, N, and O chemical topographies are directly linked to the structural backbone of plant substructures. Zn, Fe, Na, Mg, Al, and P were linked to globoid structures within protein storage vacuoles with variable levels of co-localization. Si distribution was atypical, being contained in the aleurone apoplast and symplast, supporting a physiological role for Si in addition to its structural function. These results reveal that the immobilization of metals within the observed endomembrane structures presents a structural and functional barrier and affects bioavailability. The combination of high spatial and chemical X-ray microscopy techniques highlights how *in situ* analysis can yield new insights into the complexity of the wheat aleurone layer, whose precise biochemical composition, morphology, and structural characteristics are still not unequivocally resolved.

Key words: Aleurone, aluminium, full-field imaging, globoids, phosphorus, scanning X-ray microscopy, silicon, wheat, X-ray fluorescence, zinc.

Introduction

Humans need at least 22 elements for their well-being, which can be supplied by an appropriate diet. Edible grains are the staple food for many people, and improvements in the mineral content in cereal products provide a basis for a potential strategy to improve human nutrition. The major essential inorganic nutrients required for human and animal life that are frequently lacking in diets are Fe, Zn, and Mg (White and Broadley, 2005). The highest concentrations of mineral elements within wheat (*Triticum aestivum*) seed are found in the outer endosperm cell layer, which is differentiated into the aleurone. Several molecules of nutritional interest were reported to be concentrated in the contents of

Abbreviations: DPC, differential phase contrast; EM, electron microscopy; EDXMA, energy-dispersive X-ray microanalysis; ER, endoplasmic reticulum; FFIM, full-field imaging mode; LEXRF, low-energy X-ray fluorescence; micro-PIXE, micro particle-induced X-ray emission; PSV, protein storage vacuoles; SR, synchrotron radiation; LEXRF, low-energy X-ray fluorescence; SIMS, secondary ion mass spectrometry; SXM, scanning X-ray microscopy; XAS, X-ray absorption spectroscopy; ZP, zone plate.

aleurone cells (vitamins, minerals, etc.), and other molecules (dietary fibres, phenolic acids, etc.) may be associated with aleurone cell walls and other peripheral tissues (Antoine *et al.*, 2004). The storage function of aleurone cells in cereals involves the accumulation of high levels of protein (46% w/w) and phytic acid (40% w/w) (Urbano *et al.*, 2000; Bohn *et al.*, 2007). Phytic acid is the main P storage compound in most seeds. It is a strong chelating agent that readily binds metal cations such as Ca, Zn, Mg, Fe, and Mn, making them insoluble and thus unavailable as nutritional factors, resulting in a decrease in their bioavailability in food (Lönnerdal, 2000; Urbano *et al.*, 2000; Jiang *et al.*, 2001; Ficco *et al.*, 2009). These phytic acid complexes are concentrated in electron-dense parts of the protein storage vacuoles (PSVs) of aleurone cells, referred to in older literature as phytate globoids. The term used to describe the globoids has not been generalized; they are found in the literature as a synonym of aleurone grains or protein storage bodies (Becraft, 2007; Brown and Lemmon, 2007). In this study, the term globoids will be used when referring to aleurone storage grains.

Vacuoles perform a multitude of cellular functions including the maintenance of cell rigidity and integrity, the turnover of macromolecules and the sequestration of toxic compounds and secondary metabolites, degradation of cellular components, and accumulation of reserve proteins (Marty, 1999). The presence of both lytic (<10 μm) and protein storage compartment (>10 μm) vacuole types was confirmed in barley aleurone cells by light and fluorescence microscopy studies (Swanson *et al.*, 1998). In wheat, the PSVs are composed only of a protein matrix and globoids with phytic acid mineral salts (Morrison *et al.*, 1975). This partitioning of storage and lytic functions within the same cell may reflect the need to keep the functions separate during development and maturation, and provide the digestive enzymes necessary for degradative processes during germination (Jiang *et al.*, 2001; Becraft, 2007).

The understanding of differences in the composition of the substructures of the grain, and particularly in the distribution of functionally and nutritionally important components, is important if the technological value of the grain needs to be optimized. Therefore, the aleurone layer constitutes a complex tissue to investigate. Elemental allocation at the level of the whole seed, and more precisely at the level of the individual cell and its structures, is being considered with increasing interest. This goal might be achieved by direct chemical element imaging, which enables tissue distribution to be linked with biochemical functions (Takahashi *et al.*, 2009). Element localization methods such as microparticle-induced X-ray emission (micro-PIXE) provide unique information on spatial element distribution and its concentration, but their drawbacks are poorer lateral resolution and insufficient access to the lighter (low-Z) elements (Vogel-Mikuš *et al.*, 2007, 2008). On the other hand, energy-dispersive X-ray microanalysis (EDXMA) combined with electron microscopy (EM) is less sensitive due to a much higher continuous background (Nečemer *et al.*, 2008). Secondary ion mass spectroscopy (SIMS) requires sample fixation and embedding in resin (Mills *et al.*, 2005; Larré *et al.*, 2010), possibly affecting the elemental distribution. The value of synchrotron-based low-energy X-ray fluorescence (LEXRF) in the area of simultaneous elemental distribution detection with submicrometre resolution and parts per million accuracy has been widely demonstrated (Kaulich *et al.*, 2009; Punshon *et al.*, 2009). LEXRF is particularly suited to analyse the elemental structural organization of cellular compartments. The C-based skeleton of the cell, composed of very low-Z elements (C, O, and N), can be assessed together with macro- or microelements such as Zn, Fe, Na, Mg, Al, Si, and P to reveal the physiological and structural environment of elemental distribution. However, the effects of dehydration, preservation, and sectioning, as well as X-ray self-absorption effects for lower energies, have to be taken into account. The sample preparation is therefore the crucial step for a proper analysis, and the thickness of the cross-sections investigated in this work was carefully selected to minimize all these possible side effects. The X-ray full-field imaging mode (FFIM) and scanning X-ray microscope (SXM) were used to resolve the ultrastructures of the aleurone cells, especially the aleurone grains or globoids, and to determine their associated element content using LEXRF. These techniques allow analyses to be carried out directly on the tissue samples, combining information on topographical distribution with chemical analyses without any use of immunolabelling or antibody methods. The combination of these two X-ray microscopy techniques bridges the gap to the plethora of other analytic techniques in terms of morphological characterization, spatial lateral resolution, and chemical sensitivity (Kaulich *et al.*, 2006).

Materials and methods

Plant material and sample preparation

Wheat (*Triticum aestivum* L.) cv. Reska was sown on the experimental field of the Biotechnical Faculty, University of Ljubljana, Ljubljana, Slovenia (320 m above sea level, 46°35'N, 14°55'E) on 10 October 2007. Mature grains were collected from the plants on 24 July 2008, and air dried.

The grains were soaked in deionized water overnight and cut in half with a sharp stainless steel razor. The halves were transferred into aluminium foil beds (0.5×0.5×0.5 cm) filled with a drop of deionized water, and dipped into liquid nitrogen. These frozen samples were then transferred into a cryomicrotome (Leica CM3050, Nussloch, Germany) chamber where they were glued to a sample holder with tissue-freezing medium (Jung, Leica Microsystems, Nussloch, Germany) to ensure the stability of the sample during cutting.

Cryosectioning of 10 μm thick sections was performed at –25 °C using disposable stainless steel cryomicrotome blades. The cross-sections were examined using a dissecting binocular attached to the cryomicrotome, and placed on a pre-cooled filter paper in specially designed pre-cooled aluminium beakers with covers. To ensure the flatness of the sections, they were covered with another pre-cooled filter paper and fixed with a pre-cooled heavy object (e.g. part of a microscope object glass). Specimens were transferred in liquid nitrogen to an Alpha 2-4 Christ freeze-dryer (Martin Christ Gefriertrocknungsanlagen, Osterode, Germany) and freeze-dried at –30 °C and 0.340 mbar for 3 d. The thickness of the cross-section

was set to 10 μm in order to preserve the intact morphology and element distribution of the sample, so that it could be self-standing and easily handled, as well as to ensure a good X-ray transmission signal. The freeze-dried samples were mounted onto folding golden grids (Agar Scientific, Stansted, Essex, UK) and kept in a desiccator together with silica gel until analysis.

Synchrotron radiation soft X-ray spectromicroscopy

The experiments were carried out at the TwinMic beamline at the Elettra synchrotron radiation facility in Trieste (www.elettra.trieste.it). TwinMic is a soft X-ray transmission and emission microscope (Kaulich *et al.*, 2006) operating in the 400–2200 eV photon energy range. This instrument combines complementary microscopic modes using versatile contrast techniques, such as brightfield and differential phase contrast (DPC) imaging (Morrison *et al.*, 2006), and spectromicroscopic capabilities such as X-ray absorption spectroscopy (XAS) and LEXRF with a submicrometre spatial resolution.

High-resolution imaging with FFIM

High optical resolution images were acquired in the FFIM, which is the X-ray analogue to a conventional visible-light transmission microscope. In an FFIM, monochromatic light from an X-ray source is condensed onto the specimen by focusing diffractive optical elements, the so-called zone plates (ZPs). The image of the specimen is magnified by a second ZP acting as an objective lens into a spatially resolving detector used as a CCD camera. The objective lens used for the experiments has a diameter of 100 μm, a diffraction-limited optical resolution of 18 nm, and was manufactured at the Paul Scherrer Institute, Villigen, Switzerland (Jefimovs *et al.*, 2007).

Low-energy X-ray fluorescence analysis with scanning mode (SXM)

The SXM operates similarly to a scanning electron microscope. A microprobe is formed by a ZP lens and the specimen is raster scanned across it.

The SXM is well adapted to elemental and chemical analysis as it allows multidetector geometries and simultaneous acquisition of X-ray transmission and photon or electron emission signals. The low X-ray energy range is particularly suited for bio- or physiological investigations, allowing the simultaneous acquisition in fluorescence mode of the elemental distributions of low-Z elements (from B to P from the K emission lines) as well as higher Z elements (from Ca to Nb from the L emission lines). For the experiments described here, a configured transmission detector system was used in combination with a LEXRF set-up. The configured detector set-up consists of a fast read-out electron-multiplied CCD camera coupled to an X-ray to visible light converting system. This set-up allows simultaneous acquisition of the absorption and DPC information. Special tuning of the SXM and the edge enhancement in DPC can provide 3D-like DPC X-ray micrographs, providing a wealth of additional information to the FFIM images.

In addition to the transmission signals, the element-specific LEXRF signals were acquired from trace elemental constituents in the specimen. The LEXRF set-up used for this experiment consists of an annular arrangement of Si drift detectors (PNSensor, Munich, Germany) coupled to read-out electronics (Alberti *et al.*, 2009; Gianoncelli *et al.*, 2009). This fluorescence set-up currently allows only qualitative analyses, although the implementation of fully elemental quantification is ongoing and will be the subject of future communications.

Data analysis

The superior quality of the FFIM X-ray micrographs allows raw data to be published without flat-field or background correction. The grey level histogram is adapted to better visualization of image details. The DPC or absorption image as well as the elemental cartographies obtained in scanning mode of the TwinMic microscope were normalized with respect to the exponential decrease of the electron beam current of the storage ring. The X-ray beam fluctuations were corrected by using linear fit algorithms known from atomic force microscopy.

The X-ray fluorescence spectra obtained for each pixel in the raster scan were batch processed by fitting the peaks with a Gaussian model and with a linear or polynomial baseline subtraction, using the PyMCA data analysis software (Sole *et al.*, 2007). This computation takes into account various parameters of the analysis conditions, such as the absorption of the X-rays by the optical components in the beam path, the distance between the sample and the detectors, fluorescence yields, photoionization efficiencies, or self-absorption. Elemental maps were generated by plotting the intensity of fluorescence peaks as a function of their sample position in the focal plane.

Results

The aleurone cells in wheat are cuboidal in shape, with a mean length of ~50 μm and relatively thick walls. The sample preparation ensures the preservation of the morphology of all the tissue layers in the region selected, as is visible in Fig. 1.

Full-field X-ray microscopy images of aleurone cells

The images acquired in the FFIM reveal the structures comprising an aleurone cell (Fig. 2). The size and shape of the aleurone cells were not uniform throughout the whole grain (Fig. 1), but their inner structures are characteristic and common to all parts of the grain.

At maturity, the cell walls of the aleurone layer consist of two distinct layers that differ in their X-ray absorption properties, and thus in their chemical and physical properties: the outer cell wall and the inner cell wall (Fig. 2A). These walls are pitted and show an irregular thickness in accordance with their position in the aleurone layer. The outer cell wall is a light X-ray-absorbing structure, indicating its fibrilar composition, whereas the inner cell wall

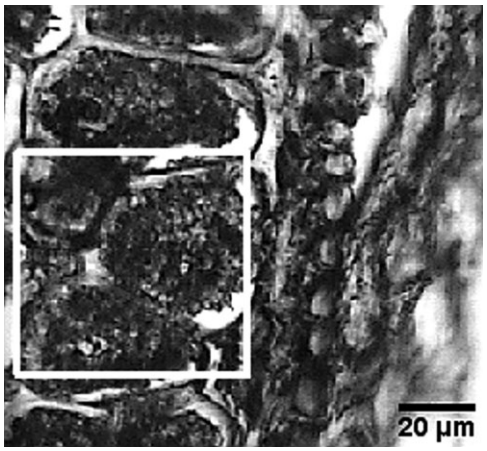

Fig. 1. Structures of a wheat grain in cross-section, obtained by optical microscopy after cryofixation, sectioning, and freeze-drying. The region of interest raster scanned with the TwinMic X-ray spectromicroscope is indicated.

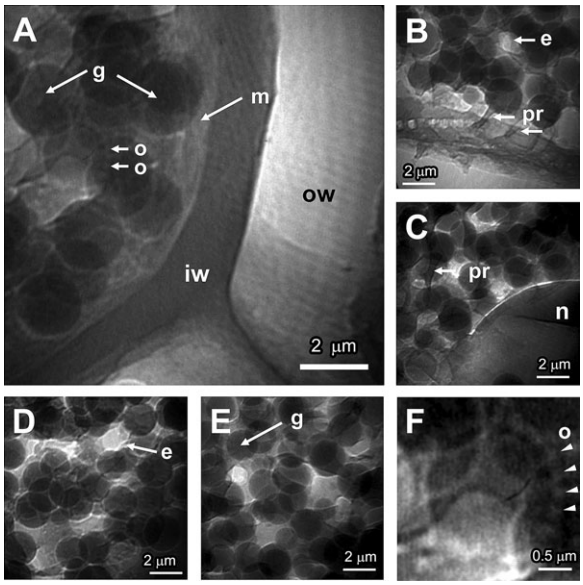

Fig. 2. High-resolution X-ray micrographs of the wheat aleurone layer acquired in full-field transmission imaging mode (FFIM) with an incident photon energy of 720 eV and 1 s acquisition time and with a 18 nm diffraction-limited optical resolution zone plate. (A) Aleurone grains and cell structures. (B) Globoids with protrusions and membrane structures. (C) Nucleus surrounded by globoids. (D, E) Globoids, endosome, and embedding matrix. (F) Oleosomes surrounding one of the globoids. e, endosome; g, globoids, m, plasma membrane; n, nucleus; o, oleosome; ow, outer cell wall; pr, protrusions; iw, inner cell wall.

is thinner and appears denser and more homogeneous in its composition. The forming walls exhibit a distinct gradation with a terminus of fusing vesicles linked to the plasma membrane or lamellar/tubular structures (Fig. 2B), and are adjacent to the plasma membrane (Fig. 2A).

Apart from distinctive cell walls, mature aleurone cells are characterized by prominent nuclei and aleurone grains or globoids (Fig. 2). The nucleus appears quite X-ray absorbing despite its inherent chemical composition. Its separative membrane, the nuclear envelope, is easily visible on the X-ray transmission images with its translucent and refractile appearance, isolating the nucleus from the cytoplasm and protein matrix in which the globoids are embedded (Fig. 2C).

The spherical, densely packed globoids constitute the most prominent organelles in the cell. Their arrangement within the aleurone cell is apparently random (Fig. 2D, E), and the relationship of that assembly to the gross structure of the aleurone cell is shown in Fig. 2A and B. The globoids are embedded in a 3D porous network of granular appearance, of lower X-ray absorption and density, forming a matrix that occupies the intergloboid spaces (Fig. 2B, D) and fills the aleurone cells.

Additionally, near the plasma membrane (Fig. 2B, C), roughly cylindrical protrusions of ~200 nm in diameter and up to 2 μm long are present within and between the matrix, globoids, and membrane structures. They are especially visible when later confluent with the surface or the walls of the aleurone cell. Nevertheless, the possibility that these protrusions belong to the endoplasmic reticulum (ER) cannot be discarded. Therefore, it is difficult, despite the projections of the 3D information onto the 2D images presented here, to be more specific about their possible interconnections and relationships with other cellular membrane structures.

Finally, some brighter features of irregular forms, possibly endosomes, are visible, especially in the proximity of cell walls, providing uneven separations between the globoids inside the cytoplasm (Fig. 2A–C).

The average sizes of globoids typically range from ~1 μm to 2 μm. The content of these X-ray-dense vesicles appears homogeneous, but diverse X-ray-absorbent vesicles present a range of various X-ray absorption densities. These densities are not systematically proportional to the diameter of the globoids and probably relate more to their biochemistry (Fig. 2B, D, E). These globoids present well-defined edges surrounded by a membrane, the tonoplast, which is clearly indicated by a bright halo. This is a less X-ray-absorbing circle around the vesicles, indicative of their different compositions, and is probably of cytoplasmic nature. Additionally, the globoids do not seem to be linked to each other. Moreover, although difficult to see because of their translucent nature and tiny spherical size <100 nm on average), small lipid bodies called oleosomes surround the globoids (Fig. 2F). They are also particularly located in the vicinity of the aleurone cell walls, where they are clearly visible, sometimes separately from the globoids, and can be present in larger sizes, ranging from 100 nm to 300 nm.

Elemental distribution of the aleurone layer revealed by LEXRF analysis

The DPC image (Fig. 3, DPC) reveals the different structures and substructures comprising the area of the aleurone which can be recognized and linked to the visible light image (Fig. 1). This provides the geochemical framework in which essential elements are deposited in the aleurone layer. Figure 3 reports the generated maps of C, O, N, Na, Mg, Al, Si, P, Fe, and Zn.

The maps of C, O, and N are representative of the structural skeleton of the aleurone cells investigated. These are the primary elements involved in the formation of aleurone cell structures, and comprise major building macromolecules such as carbohydrates, proteins, and lipids. These elemental maps, as expected, show high contributions in cell walls. Relatively more C is present inside the apoplast region, whereas O and N are higher in the symplast region, inside the plasma membrane of the aleurone cell. The repartition of O and N in the aleurone cell substructures is fully correlated, although the signal of N is proportionally significantly lower. O and N distributions inside the aleurone cells coincide with the localization of the aleurone grains or globoids, as revealed by the phase contrast image (Fig. 3, DPC). However it is worth to mention that a residual signal persists in the entire symplast region, and is

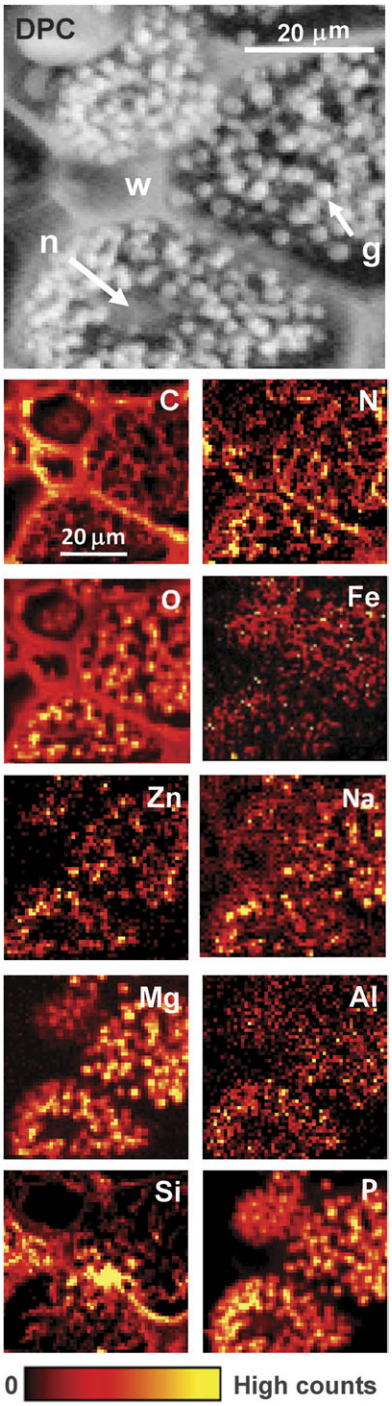

Fig. 3. Differential phase contrast X-ray micrograph (DPC) of wheat aleurone cells with aleurone globoids (g), cell nucleus (n), and cell wall (w). Simultaneously acquired low-energy X-ray fluorescence (LEXRF) maps of C, N, O, Fe, Zn, Na, Mg, Al, Si, and P. To maximize the photon absorption cross-section and the count rate, two different incident photon energies were used: E=1686 eV for C, O, Zn, and Na, and E=2172 eV for Mg, Fe, Al, Si, and P. The maps were collected over a field of view of 58 μm×58 μm, as a 58×58 pixel raster scan, a dwell time of 8 s pixel^{-1}, and with a probe size of 0.76 μm. The scale bar is in arbitrary units.

probably linked to the cytoplasm and the embedded matrix of the globoids seen on the high-resolution images (Fig. 2).

Elemental microanalysis of the aleurone cells revealed that Zn, Fe, Na, Mg, Al, and P appear to be distributed in a similar way: their highest proportions are contained in the globoids of the symplast region of the aleurone cells. It is especially clear that the globoids are the sites of relatively high P concentration, and that there is little P in the cell walls. The same can be observed for Mg. Therefore, the elemental cartographies of P and Mg, due to the higher fluorescence signal, demonstrate a positive correlation of their distributions, specifically inside the globoids. This co-localization is also globally valid for the spatial distributions of Zn, Fe, Na, and Al, which follow the repartition of P and Mg. However, a small discrepancy can be noticed on the Na map, which shows a presence inside the walls of the aleurone cells in addition to the above-mentioned localization.

Finally, the distribution of Si differs significantly from that of the majority of the elements observed, being deposited in a high proportion inside the cell walls. Si is also present inside the aleurone cells, but does not seem to be contained exclusively in the globoids. Its distribution also appears rather homogeneous inside the cytoplasm of cells.

These maps also reveal some differences in the elemental composition and relative proportion between globoids belonging to the same or to adjacent cells. Indeed, the relative intensities of the globoid contents differ from one part of the symplast to another. The relative distributions of Mg, Zn, or Al, for instance, or Si, vary from one tiny area to another, evidence of the biochemical spatial heterogeneity within the symplast of the cell. Because the micro X-ray beam penetrates the sample to its entire depth, the signal emitted by the sample and collected by the detectors comes from a small volume; it is therefore difficult to state that this observation can be extended to differences between single globoids. However, this trend in chemical composition difference found between a sample of average aleurone grains is likely to occur at a smaller scale.

Discussion

Electron microscopy has been extremely successful in revealing the subcellular organization at an impressive level of resolution. It has reached the point that present knowledge of plant cellular organization is based mainly on EM studies (Gunning and Steer, 1996). However, EM has an important limitation in that other than for observations of whole cells, it is limited to very thin layers and heavily depends on accurate sample preparation. Thanks to the penetration power of X-rays, entire cells or cellular layers can be probed with an easier sampling, because thicker slices—with respect to EM—can be investigated. The FFIM of the TwinMic X-ray microscope offers ideal conditions to probe the microstructures of aleurone cells, especially aleurone grains. It offers a new approach for high-resolution imaging of plant seeds.

Aleurone cell walls of wheat are composed primarily of β-glucans and arabinoxylans, with small amounts of glucomanan and cellulose also present. The walls are made of several layers, as previously described (Bacic and Stone, 1981), and can be clearly distinguished on high-resolution X-ray micrographs (Fig. 2A). The outer wall zone is thicker, exhibiting a multilammellar pattern, and is degraded rapidly during germination. The inner wall, which is extremely rigid, lies adjacent to the plasma membrane, is thin, resistant, and persists during early stages of germination (Bacic and Stone, 1981; Fath *et al.*, 2000; Robert *et al.*, 2010). Differences in their composition revealed by imunolabelling indicate a higher portion of arabinoxylans, which may be esterified by ferulic acid to various degrees, in the inner wall, whereas the outer wall is richer in β-glucans (Guillon *et al.*, 2004). However, the relative distribution of their constitutive polymers still needs to be properly addressed. The high degree of polymerization of the inner wall and the numerous cross-links between its constitutive molecules explain the higher density and therefore the difference in X-ray contrast observed. For both layers, the polysaccharide network presents sufficient interfibrillar and intermicellar spaces so as not to constitute a major diffusion barrier for molecules (Sattelmacher, 2001). Nevertheless, their residual negative charges may lead to an accumulation of some ions, as reflected in the LEXRF results and discussed later.

Globoids of up to 2 μm and of differing densities filling the aleurone cells were observed by high-resolution imaging. Single PSVs can also have a composite structure containing the globoids, with biochemical characteristics of a lytic vacuole embedded in a protein matrix, thus comprising a vacuole within the vacuole (Jiang *et al.*, 2001; Vitale and Hinz, 2005). It is suggested by high-resolution images that at maturity, some globoids from aleurone cells have direct tubule-shaped protrusions from their membranes to the endomembrane structures and appear as if they were formed by budding from this common cisternae-shaped formation. No further membrane boundary is visible and the globoids appear to be individually separated, in agreement with the reports which found that once formed, the globoids can either remain attached to the ER or bud off as separated organelles (Herman and Larkins 1999). In wheat, globoids do not remain as separated organelles but are sequestered into provacuoles (Rubin *et al.*, 1992), which can fuse to one another and form at least one large central PSV containing many globoids. These data suggest that only a few—maybe even only one—large central vacuoles exist in wheat and contain all the globoids, because no other membrane structure was visible in the full-field images. Moreover, the globoids are surrounded by oleosomes, small spherical X-ray-refractile bodies embedded within the tonoplast. They are the site of neutral lipid storage, mainly triglycerides, as was demonstrated in barley cells (Bethke *et al.*, 1998). It is commonly accepted that triglycerides are synthesized on ER membranes and deposited in oleosomes, so the presence of these structures provides valuable additional information about the ER origin of the globoids in wheat.

A direct correlation between the amount of phytic acid in the seed grain and the size of the globoids has been reported (Bohn *et al.*, 2007). As phytic acid is an effective chelator of cations, the amount and affinity to link these metals depend on the phytic acid concentration available, and therefore differential deposition is likely to occur within aleurone grains. All these particular substructures define specialized and membrane-isolated environments (Jiang *et al.*, 2001) that are required to perform certain functions. The size of the globoids and their X-ray absorption contrast are highly variable, indicating differences in their function on this small scale. These PSV multicompartmentalizations protect the organelle's physiochemical integrity from any interference coming from ongoing processes in other organelles and enhance the complexity of the intracellular pathways.

The LEXRF results link these purely structural investigations with the elemental profiles and are in accordance with numerous studies that have revealed, for different types of seeds, two major sites of metal ion fixation in the aleurone layer: the aleurone grains or globoids and the walls. The globoids belongs to PSV categories. The main characteristic of PSVs is that stored materials accumulate either as large polymers, which is the case for stored C and N, or as complex salts, which is the case for sequestered minerals (Bewley and Black, 1994) and proteins (Cakmak *et al.*, 2004). As for cell walls, their physicochemical properties influence plant mineral nutrition and elemental distribution, as metal ions do not simply pass through the apoplast to the plasmalemma, but can also be adsorbed or fixed to cell wall components. The movement of ions in cell walls is also partially dependent on electrostatic interactions leading to an accumulation of cations in apparently free space of the wall (Sattelmacher, 2001).

The potential of the LEXRF technique for the study of the aleurone layer was previously established as a purely descriptive example for studying the distribution of some of the elements reported here, but without entering into the physiological aspects and implications of the elemental distributions in wheat (Kaulich *et al.*, 2009). Moreover, without the valuable morphological information gained with the high-resolution imaging on the same aleurone cells, it was not possible to establish a link between the particular subcellular components, the elements, and their possible functions. The C-based skeleton of the aleurone cells, representative of the different structural features, is perfectly visible on the elemental maps of C and O, and to a lesser extent on that of N, and can easily be superimposed on the X-ray absorption image. Visible in the different elemental cartographies, and clearly visible from the Si map, it was found that walls contain many cations, but are relatively richer in C, O, and Si. The symplast of wheat aleurone cells contains proportionally more O, N, Na, Fe, Zn, Mg, Al, and P. This is in accordance with energy-dispersive X-ray (Lott, 1984) and SIMS (Heard *et al.*, 2002; Mills *et al.*, 2005) analysis of globoids from different tissues and species that have shown the presence of P, Mg, and K, with occasional storage of Ca, Mn, Na, Zn, Ba, and Fe.

Si is not considered to be an essential element for higher plants as it has no nutritional value, but it is well known that Si is beneficial for the healthy development of many plants (Epstein, 1999). The LEXRF map of Si clearly shows a preferential localization in the walls, with some hot-spots of Si accumulation. However, a non-negligible proportion is also found in the cytoplasm of the aleurone cell, as was reported for barley (Ockenden *et al.*, 2004). The chemical elements Si, Ca, and Mn have been reported to accumulate in a spatial arrangement with autofluorogens, which are phenolic compounds related to lignin biosynthesis (Carver *et al.*, 1998). Si may complex with various organic constituents, and polymerizes easily to form silica gel (SiO_2, nH_2O) (Ma and Yamaji, 2006). With its four active valences, Si can form chemical bonds almost as readily as C. Si can be covalently combined with alginic and pectic acids, some polysaccharides, and proteins. This means that Si requires only a small quantity of available phenolics or other organic compounds to undergo conversion to insoluble, localized deposits in cell walls and cellular substructures. The easy precipitation of Si also leads to its occurrence in transpiration termini (Raven, 1983). The biogenic Si structure is affected by ambient physicochemical conditions mediated by tissue maturation, pH, ionic concentrations, and cell wall structure. Si deposits, commonly called phytoliths, have been reported to occur in cell walls, the cell lumen, and in extracellular locations in the roots and the shoot, including leaves and culms, and in the inflorescence of wheat (Sangster *et al.*, 2001). Some other inclusions, of SiO_2 crystals for instance, can be found suspended in the cytosol and can occur within or outside cell walls (Prychid *et al.*, 2003). Silicified tissues are believed to provide plant support and protection, and may also sequester toxic metals, as shown by the co-deposition of Al with Si in cereals and conifers. It has been proposed that Si mitigates the toxicity of Al in wheat (Cocker *et al.*, 1998) to alleviate abiotic stresses effectively in higher plants. From the co-localization of Si and Al in *Picea* needles, it was concluded that the formation of extracellular insoluble Al/Si compounds was responsible for the amelioration effects. However, in other experiments, no Al was detected in cellular Si precipitates (Hodson and Sangster, 1990; Neumann and zur Nieden, 2001). The observed localization of Al in the content of aleurone cells in wheat does not support a total or clear positive co-localization of Al and Si. Therefore, the present data strongly support the evidence that Si is not only a cell wall incrustation responsible for the rigidity of the cell structures, but is also involved in physiological processes (Epstein, 1999).

On the other hand, the results strongly support the co-localization of Al and P, which, according to our knowledge, represents a novelty in seeds. The binding of Al to P, probably in the form of $Al_4(PO_4)_3$, has been seen in the root cell walls of buckwheat, oat, and maize, and was shown to help delay Al uptake by the cytosol and therefore improve plant resistance to Al (Zheng *et al.*, 2005). Moreover, the binding of Al to excreted organic acids confers the primary mechanism of Al resistance in plants (Mossor-Pietraszewska, 2001). In wheat, high Al resistance was attributed to *Triticum aestivum* Al-activated malate transporter (TaALMT1) (Delhaize *et al.*, 2007; Ma, 2007). In the cytosol, Al tends to bind to the phosphate or carboxyl groups, rather than to the -SH groups (Mossor-Pietraszewska, 2001). However, this process is far from being understood. Some uncertainties also remain about the pathway of Al transport in the seed, where it was found to be stored in the globoids in the present experiment. As phloem sap contains very high concentrations of P (Marschner, 1995), P may represent a suitable ligand for Al in phloem and for its final loading into the seeds. However, further investigations are needed to confirm this hypothesis.

Of the other minerals, Fe is of interest because of its central roles in improving crop yields and in human nutrition (Jeong and Guerinot 2009). Still, mechanisms of subcellular compartmentation of iron in graminaceous plants are poorly understood. LEXRF maps reveal that most of the Fe is found in the symplast of aleurone cells and relatively lower amounts may be present in the apoplast. In walls, Fe may roughly account for concentrations an order of magnitude lower than in the symplast, and may be remobilized under specific conditions (Zhang *et al.*, 1995). Due to it lower relative amount, however, the release of Fe from the apoplast presumably represents a rather negligible source for Fe remobilization. It is known that in seeds, Fe may be complexed as ferritin or phytic acid mineral salt (Nozoye *et al.*, 2007). Ferritins can store up to 4500 iron atoms in their central cavity. They are preferentially localized in plastids and were widely accepted as predominant Fe stores (Jeong and Guerinot, 2009; Briat *et al.*, 2010). Phosphate availability, on the other hand, was found to be related to accumulation of phosphate–Fe complexes in the vacuoles of *Arabidopsis* leaves. The vacuoles were reported to largely accommodate Fe, when present in excess. Under phosphate deficiency, however, most Fe was found inside the chloroplasts, most probably associated with ferritins (Pich *et al.*, 2001; Hirsch *et al.*, 2006). The present results support the strong interdependence of Fe and P, and reinforce the role of globoids as primary stores of Fe. Primary functions of globoids in wheat aleurone cells are mineral accumulation, long-term storage, and subsequent remobilization of elements at onset of germination. To sustain those functions, both morphological and biochemical optimization of the structures are needed, and it seems likely that Fe complexation with phytic acid may be more cost-efficient than ferritin biosynthesis. The comparison of LEXRF maps with the DPC image indicates that most of the Fe in symplasts is co-localized with Zn, Al, Mg, and P in globoids of aleurone cells. Although nicotianamine (NA) is acknowledged as the primary chelator for seed delivery, vacuolar storage, and Fe remobilization, the same role may also be assigned to organic acids. In addition, both types of molecules are involved in the binding and distribution of Zn, but also other divalent cations such as Mg, Mn, and Cd (Duggleby and Dennis, 1970; Evans, 1991; Pich *et al.*, 2001; Takahashi *et al.*, 2009; Kobayashi *et al.*, 2010). The understanding of Fe homeostasis in grasses may

therefore also be of importance for biofortification of Zn, and possibly other cations. Furthermore, soil heavy metals may profoundly influence Fe availability, transport, distribution, and utilization, whereas Fe deficiency may modify heavy metal uptake and accumulation (Fodor, 2006). Both processes may significantly affect the seed mineral and unwanted metal constitution. Taken together, the present data on characterization of aleurone cells in wheat support the role of globoids as central morphological, structural, and biochemical features, presumably affecting mineral accumulation, storage, and remobilization. An integral approach to iron uptake, transport, storage, and remobilization mechanisms will therefore be needed before further progress can be made in seed iron biofortification.

Zn is a micronutrient essential for all organisms. It is required as a cofactor in >300 enzymes and plays critical structural roles in many proteins, including countless transcription factors (Palmgren *et al.*, 2008). However, Zn can also be toxic when present in excess, and the physiological and physical range between the deficiency and toxicity concentration of Zn is narrow. Consequently, a tightly controlled metal homeostasis network that can adjust for Zn concentration and availability is a necessity (Maret and Sandstead, 2006). If unregulated, the high affinity binding of Zn to S-, N-, and O-containing functional groups in biological molecules, as well as uncontrolled displacement of essential cofactor metal cations such as Mn and Fe, or enzymatic and P carriers such as Mg, can cause damage. Indeed, Zn is not redox active. This property, combined with the pronounced Lewis acid characteristics of the Zn^{2+} ion and the flexibility of the co-ordination sphere with respect to possible geometry and ligands, helps to explain why the functionalities of Zn inside one cell are so extensive. Zn has been shown to accumulate in the total endosperm not only with phytic acid, but also with proteins (Cakmak *et al.*, 2004). The LEXRF maps demonstrate a positive correlation between Zn and P, N, C, and O inside the symplast of aleurone cells, but also with Mg and Al, supporting these hypotheses. However, investigation of the ligands involved in this storage pattern is required in order to be more specific.

High levels of P are found in aleurone cells, mainly in the globoids as revealed by the correlation of the X-ray absorption map showing these aleurone substructures and the LEXRF (Fig. 3). The majority of P (80%) in wheat grain is in the form of phytic acid, which is stored mainly in aleurone cells (Bohn *et al.*, 2008). In wheat, phytic acid has been shown to co-localize with K, Ca, Mg, and Na (Mills *et al.*, 2005). However, phytic acid binds strongly to other metallic ions such as Mn, Zn, Fe, Al, or Si via ionic associations (cross-linking) with negatively charged phosphates (Lott, 1984) to form an insoluble mixed salt that immobilizes the P and the mineral reserves for nutrition purposes. The order of ability of mineral cations to form complexes with phytic acid *in vitro* is $Cu^{2+} > Zn^{2+} > Ni^{2+} > Co^{2+} > Mn^{2+} > Fe^{2+} > Ca^{2+}$ (Bohn *et al.*, 2008). One of the approaches to counteract the negative effects of phytic acid in seeds and grains used for food has been the selection of low phytic acid genotypes that have approximately normal P concentrations. A decrease in average size and an increase in the number of aleurone globoids, which are up to 3 μm in diameter in wild-type wheat, was seen for the grain of low phytic acid wheat, which retains its ability to incorporate minerals, mainly P, K, and Mg. Joyce *et al.* (2005), using STEM-EDX, did not report any large differences in mineral concentrations and distributions between the wild type and the low phytic acid wheat Js-12-LPA. This indicated no direct role for localization of phytic acid and mineral distribution, but rather a chelating effect of the phosphate groups. Similar results were also observed for low phytic acid maize plants (Lin *et al.*, 2005). However, this engineering of the chemistry of the grain P, especially at the storage sites, requires a close follow-up of its related elemental framework. The present study constitutes a first step towards better understanding of the physiological storage abilities of the aleurone layer. Consequently, comparison of full-field imaging with LEXRF globoid structures allows the conclusion to be drawn that the great majority of the elements P, Mg, Na, Fe, Zn, Al, and Na present in wheat aleurone cell cytoplasm are located inside these globoid deposits. Clearly separated hotspots of these elements can be appreciated on the elemental maps, within the globoid structures (Fig. 3). More precisely, the distributions of P, Fe, Zn, and Mg in wheat aleurone cells showed positive and unique correlations to each other, which give strong indications about their interconnection. The factors governing metal selectivity in phytic acid mineral salts are unclear, possibly involving differential mineral availability, uptake, and deposition rates. Thus, the levels and distribution of metal species are not necessarily homogeneous even within single globoids (Lott, 1983). Furthermore, globoid size, content, and distribution within cells are heterogeneous, and globoid bodies may look structurally similar and have distinctly different elemental storage characteristics (Witkowski *et al.*, 1997). This was shown by the present high-resolution imaging study, which revealed the presence of different densities, linked to different chemical composition, and which is in agreement with the fluorescence spectra acquired, as well as with the elemental maps presented in this work. These results suggest that the complexity and morphological, structural, and physiological dynamics of plant cells cannot be explained merely by physicochemical characteristics, and that detailed *in situ* localization methods at the cellular and subcellular levels are essential for studies in plant biology. This work strengthens the idea that besides the binding ability of phytic acid, the structural organization of globoids contributes to the immobilization of mineral elements in aleurone cells; the differences in metal distribution might suggest differences in their storage form. However, further analyses are required to reveal the nutritional relevance of globoids as well as to link the elemental analysis to the ligands involved in the ion storage.

Conclusion

The substructures of wheat aleurone cells were assessed by FFIM and LEXRF techniques. The aleurone layer is an essential preferential storage site or, more generally an ion

metal fixation site in wheat seed for reserve N, C, and minerals. The results demonstrate in particular that the walls and aleurone globoids are the target for metal fixation and evidence for the necessity to link high level morphological studies to elemental characterization. Phytic acid, mainly located in the globoids, may contribute to the metal homeostasis process by binding to mineral elements in globoids and making them unavailable. Elemental topographical associations between Mg, Na, Al, Fe, Zn, and P were revealed in wheat aleurone grains. The distribution pattern of Si highlights the fact that the physiological and structural barrier in the unloading and uploading processes responsible for the transfer of the ions from the maternal tissues (embryo and endosperm) to the filial tissues (aleurone), together with purely storage functions, might occur independently and simultaneously in the aleurone layer. In addition, this study shows that mechanisms of nutrient immobilization and release from the globoids of the aleurone cells have to be carefully considered in future food biofortification strategies.

Acknowledgements

Professor A. Tajnšek and Dr M. Germ are acknowledged for providing the wheat cv. Reska plant material. Beam time was provided by Elettra and EU support within the framework of proposal 2008203. The experiment was performed at Elettra TwinMic beamline station. BK and AG performed the experiments and analysed the data. A scholarship from the World Federation of Scientists and a National Fellowship awarded by L'Oreal-UNESCO and the Slovenian Science Foundation to PP are gratefully acknowledged. The study was supported by the following projects: MSZS P1-0212 'Biology of Plants' Research Programme, 'Young Researchers', ARRS J4-9673, and EU COST 859.

References

Alberti R, Klatka T, Longoni A, Bacescu D, Marcello A, De Marco A, Gianoncelli A, Kaulich B. 2009. Development of a low-energy X-ray fluorescence system with sub-micrometer spatial resolution. *X-ray Spectrometry* **38,** 205–209.

Antoine C, Lullien-Pellerin V, Abecassis J, Rouau X. 2004. Effect of wheat bran ball milling on fragmentation and marker extractability of the aleurone layer. *Journal of Cereal Science* **40,** 275–282.

Bacic A, Stone BA. 1981. Chemistry and organization of aleurone cell wall components from wheat and barley. *Australian Journal of Plant Physiology* **8,** 475–495.

Becraft PW. 2007. Aleurone cell development. In: Olsen OA, ed. *Plant cell monographs. Endosperm*, Vol. 8. Berlin: Springer-Verlag, 45–56.

Bethke PC, Swanson SJ, Hillmer S, Jones RL. 1998. From storage compartment to lytic organelle: the metamorphosis of the aleurone protein storage vacuole. *Annals of Botany* **82,** 399–412.

Bewley JD, Black M, eds. 1994. *Seeds: physiology of development and germination*. New York, NY: Plenum Publishing Corporation.

Bohn L, Josefsen L, Meyer AS, Rasmussen SK. 2007. Quantitative analysis of phytate globoids isolated from wheat bran and characterization of their sequential dephosphorylation by wheat phytase. *Journal of Agricultural and Food Chemistry* **55,** 7547–7552.

Bohn L, Meyer AS, Rasmussen SK. 2008. Phytate: impact on environment and human nutrition. A challenge for molecular breeding. *Journal of Zhejiang University Science B* **9,** 165–191.

Briat J-F, Duc C, Ravet K, Gaymard F. 2010. Ferritins and iron storage in plants. *Biochimica et Biophysica Acta* **1800,** 806–814.

Brown RC, Lemmon BE. 2007. The developmental biology of cereal endosperm. In: Olsen OA, ed. *Plant cell monographs. Endosperm*, Vol. 8. Berlin: Springer-Verlag, 1–20.

Cakmak I, Torun A, Millet E, Feldman M, Fahima T, Korol A, Nevo E, Braun HJ, Ozhan H. 2004. *Triticum dicoccoides*: an important genetic resource for increasing zinc and iron concentration in modern cultivated wheat. *Soil Science and Plant Nutrition* **50,** 1047–1054.

Carver TLW, Thomas BJ, Robbins MP, Zeyen RJ. 1998. Silicon deprivation enhances localized autofluorescent responses and phenylalanine ammonia-lyase activity in oat attacked by *Blumeria graminis*. *Physiological and Molecular Plant Pathology* **52,** 223–243.

Cocker KM, Evans DE, Hodson MJ. 1998. The amelioration of aluminium toxicity by silicon in wheat (*Triticum aestivum* L.): malate exudation as evidence for an *in planta* mechanism. *Planta* **204,** 318–323.

Delhaize E, Gruber BD, Ryan PR. 2007. The roles of organic anion permeases in aluminium resistance and mineral nutrition. *FEBS Letters* **581,** 2255–2262.

Duggleby RG, Dennis DT. 1970. Nicotianamide adenine dinucleotide-specific isocitrate dehydrogenase from a higher plant. *Journal of Biological Chemistry* **245,** 3745–3750.

Epstein E. 1999. Silicon. *Annual Review of Plant Physiology and Plant Molecular Biology* **50,** 641–664.

Evans A. 1991. Influence of low molecular weight organic acids on zinc distribution within micronutrient pools and zinc uptake by wheat. *Journal of Plant Nutrition* **14,** 1307–1318.

Fath A, Bethke P, Lonsdale J, Meza-Romero R, Jones R. 2000. Programmed cell death in cereal aleurone. *Plant Molecular Biology* **44,** 255–266.

Ficco DBM, Riefolo C, Nicastro G, De Simeone V, Di Gesù AM, Beleggioa R, Platani C, Cattivelli L, De Vita P. 2009. Phytate and mineral elements concentration in a collection of Italian durum wheat cultivars. *Field Crops Research* **111,** 235–242.

Fodor F. 2006. Heavy metals competing with iron under conditions involving phytoremediation. In: Barton LL, Abadia J, eds. *Iron nutrition in plants and rhizospheric microorganisms.*. Berlin: Springer-Verlag, 129–151.

Gianoncelli A, Kaulich B, Alberti R, Klatka T, Longoni A, de Marco A, Marcello A, Kiskinova M. 2009. Simultaneous soft X-ray transmission and emission microscopy. *Nuclear Instruments and Methods in Physics Research Section A: Accelerators, Spectrometers, Detectors and Associated Equipment* **608,** 195–198.

Guillon F, Tranquet O, Quillien L, Utille J-P, Ortiz JJO, Saulnier L. 2004. Generation of polyclonal and monoclonal antibodies against arabinoxylan in cell walls of endosperm of wheat. *Cereal Science* **40,** 167–182.

Gunning BES, Steer MW. 1996. *Plant cell biology. Structure and function*. Sudbury, MA: Jones and Bartlett Publishers International.

Heard PJ, Feeney KA, Allen JC, Shewry PR. 2002. Determination of the elemental composition of mature wheat grain using a modified secondary ion mass spectrometer (SIMS). *The Plant Journal* **30,** 237–245.

Herman EM, Larkins BA. 1999. Protein storage bodies and vacuoles. *The Plant Cell* **11,** 601–613.

Hirsch J, Marin E, Floriane M, Chiarenza S, Richaud P, Nussaume L, Thibaud MC. 2006. Phosphate deficiency promotes modification of iron distribution in *Arabidopsis* plants. *Biochimie* **88,** 1767–1771.

Hodson MJ, Sangster AG. 1990. Techniques for the microanalysis of higher plants with particular reference to silicon in cryofixed wheat tissues. *Scanning Microscopy* **4,** 407–418.

Jefimovs K, Vila-Comamala J, Pilvi T, Raabe J, Ritala M, David C. 2007. Zone-doubling technique to produce ultrahigh-resolution x-ray optics. *Physical Review Letters* **99,** 264801–264805.

Jeong J, Guerinot ML. 2009. Homing in on iron homeostasis in plants. *Trends in Plant Science* **14,** 280–285.

Jiang L, Phillips TE, Hamm CA, Drozdowicz YM, Rea PA, Maeshima M, Rogers SW, Rogers JC. 2001. The protein storage vacuole: a unique compound organelle. *Journal of Cell Biology* **155,** 991–1002.

Joyce C, Deneau A, Peterson K, Ockenden I, Raboy V, Lott JNA. 2005. The concentrations and distributions of phytic acid phosphorus and other mineral nutrients in wild-type and low phytic acid Js-12-LPA wheat (*Triticum aestivum*) grain parts. *Canadian Journal of Botany* **83,** 1599–1607.

Kaulich B, Susini J, David C, *et al*. 2006. A European twin X-ray microscopy station commissioned at ELETTRA. In: Aoki S, Kagoshima Y, Suzuki Y, eds. *X-ray microscopy. Proceedings of the 8th International Conference*, Vol. 7. Tokyo: Japan, 22–25.

Kaulich B, Gianoncelli A, Beran A, Kreft I, Pongrac P, Regvar M, Vogel-Mikuš K, Kiskinova M. 2009. Low-energy X-ray fluorescence microscopy opening new opportunities for bio-related research. *Journal of the Royal Society Interface* **6,** S641–S647.

Kobayashi T, Nakanishi H, Nishizawa NK. 2010. Recent insights into iron homeostasis and their application in graminaceous plants. *Proceedings of the Japanese Academy. Series B, Physical and Biological Sciences* **86,** 900–913.

Larré C, Penninck S, Bouchet B, Lollier V, Tranquet O, Denery-Papini S, Guillon F, Rogniaux H. 2010. *Brachypodium distachyon* grain: identification and subcellular localization of storage proteins. *Journal of Experimental Botany* **61,** 1171–1183.

Lin L, Ockenden I, Lott JNA. 2005. The concentrations and distribution of phytic acid–phosphorus and other mineral nutrients in wild-type and low phytic acid 1-1 (*lpa* 1-1) corn (*Zea mays* L.) grains and grain parts. *Canadian Journal of Botany* **83,** 131–141.

Lönnerdal B. 2000. Dietary factors influencing zinc absorption. *Journal of Nutrition* **130,** 1378S–1383S.

Lott JNA. 1983. Studies of the uniformity of elemental composition in different areas of globoid crystals in protein bodies of *Cucurbita maxima* and *Ricinus communis* seeds. *Scanning Electron Microscopy* **11,** 923–928.

Lott JNA. 1984. Accumulation of seed reserves of phosphorus and other minerals. In: Murray DE, ed. *Seed physiology*, Vol. 1. New York: Academic Press, 139–166.

Ma JF. 2007. Syndrome of aluminum toxicity and diversity of aluminum resistance in higher plants. *International Review of Cytology* **264,** 225–252.

Ma JF, Yamaji N. 2006. Silicon uptake and accumulation in higher plants. *Trends in Plant Science* **11,** 392–397.

Maret W, Sandstead HH. 2006. Zinc requirements and the risks and benefits of zinc supplementation. *Journal of Trace Elements in Medicine and Biology* **20,** 3–18.

Marschner H. 1995. *Mineral nutrition of higher plants*, 2nd edn. London: Academic Press.

Marty F. 1999. Plant vacuoles. *The Plant Cell* **11,** 587–600.

Mills ENC, Parker ML, Wellner N, Toole G, Feenely K, Shewry PR. 2005. Chemical imaging: the distribution of ions and molecules in developing and mature wheat grain. *Journal of Cereal Science* **41,** 193–201.

Morrison GR, Gianoncelli A, Kaulich B, Bacescu D, Kovac J. 2006. A fast read-out CCD system for configured-detector imaging in STXM. In: Aoki S, Kagoshima Y, Suzuki Y, eds. *X-ray microscopy. Proceedings of the 8th International Conference*, Vol. 7. Tokyo: Japan: IPAP Conference Series 277–379.

Morrison IN, Kuo J, O'Brien TP. 1975. Histochemistry and fine-structure of developing wheat aleurone cells. *Planta* **123,** 105–116.

Mossor-Pietraszewska T. 2001. Effect of aluminium on plant growth and metabolism. *Acta Biochimica Polonica* **48,** 673–686.

Nečemer M, Kump P, Ščančar J, *et al*. 2008. Application of X-ray fluorescence analytical techniques in phytoremediation and plant biology studies. *Spectrochimica Acta Part B: Atomic Spectroscopy* **63,** 1240–1247.

Neumann D, zur Nieden U. 2001. Silicon and heavy metal tolerance in higher plants. *Phytochemistry* **56,** 685–692.

Nozoye T, Inoue H, Takahashi M, Ishimaru Y, Nakanish H, Mori S, Nishizawa NK. 2007. The expression of iron homeostasis-related genes during rice germination. *Plant Molecular Biology* **64,** 35–47.

Ockenden I, Dorsch JA, Reid MM, Lin L, Grant LK, Raboy V, Lott JNA. 2004. Characterization of the storage of phosphorus, inositol phosphate and cations in grain tissues of four barley (*Hordeum vulgare* L.) low phytic acid genotypes. *Plant Science* **167,** 1131–1142.

Palmgren MG, Clemens S, Williams LE, Kramer U, Borg S, Schjorring JK, Sanders D. 2008. Zinc biofortification of cereals: problems and solutions. *Trends in Plant Science* **13,** 464–473.

Pich A, Manteuffel R, Hilmer S, Scholz G, Schmidt W. 2001. Fe homeostasis in plant cells: does nicotianamine play multiple roles in the regulation of cytoplasmic Fe concentration? *Planta* **213,** 967–976.

Prychid CJ, Rudall PJ, Gregory M. 2003. Systematics and biology of silica bodies in monocotyledons. *Botanical Review* **69,** 377–440.

Punshon T, Guerinot ML, Lanzirotti A. 2009. Using synchrotron X-ray fluorescence microprobes in the study of metal homeostasis in plants. *Annals of Botany* **103,** 665–672.

Raven JA. 1983. The transport and function of silicon in plants. *Biological Reviews* **58,** 179–207.

Robert P, Jamme F, Barron C, Bouchet B, Saulinier L, Dumas P, Guillon F. 2010. Change in wall composition of transfer and aleurone cells during wheat grain development. *Planta* (in press).

Rubin R, Levanony H, Galili G. 1992. Characterization of two types of protein bodies in developing wheat endosperm. *Plant Physiology* **99,** 718–724.

Sangster AG, Hodson MJ, Tubb HJ. 2001. Silicon deposition in higher plants. In: Datnoff LE, Snyder GH, Korndofer GH, eds. *Studies in plant science: silicon in agriculture*, Vol. 8. Amsterdam: Elsevier Science, 85–113.

Sattelmacher B. 2001. The apoplast and its significance for plant mineral nutrition. *New Phytologist* **149,** 167–192.

Sole A, Papillon E, Cotte M, Walter PH, Susini J. 2007. A multiplatform code for the analysis of energy-dispersive X-ray fluorescence spectra. *Spectrochimica Acta Part B: Atomic Spectroscopy* **62,** 63–68.

Swanson SJ, Bhetke PC, Jones RL. 1998. Barley aleurone cells contain two types of vacuoles: characterization of lytic organelles by use of fluorescence probes. *The Plant Cell* **10,** 685–698.

Takahashi M, Nozoye T, Kitajima N, *et al*. 2009. *In vivo* analysis of metal distribution and expression of metal transporters in rice seed during germination process by microarray and X-ray fluorescence imaging of Fe, Zn, Mn, and Cu. *Plant and Soil* **325,** 39–51.

Urbano G, Lopez-Jurado M, Aranda P, Vidai-Valverde C, Tenorio E, Porres J. 2000. The role of phytic acid in legumes: antinutrient or beneficial function? *Journal of Physiology and Biochemistry* **56,** 283–294.

Vitale A, Hinz G. 2005. Sorting of proteins to storage vacuoles: how many mechanisms? *Trends in Plant Science* **10,** 316–323.

Vogel-Mikuš K, Pongrac P, Kump P, Nečemer M, Simčič J, Pelicon P, Budnar M, Povh B, Regvar M. 2007. Localisation and quantification of elements within seeds of Cd/Zn hyperaccumulator *Thlaspi praecox* by micro-PIXE. *Environmental Pollution* **147,** 50–59.

Vogel-Mikuš K, Simčič J, Pelicon P, Budnar M, Kump P, Nečemer M, Mesjasz-Przybyłowicz J, Przybyłowicz WJ, Regvar M. 2008. Comparison of essential and non-essential element distribution in leaves of the Cd/Zn hyperaccumulator *Thlaspi praecox* as revealed by micro-PIXE. *Plant, Cell and Environment* **31,** 1484–1496.

White PJ, Broadley MR. 2005. Biofortifying crops with essential mineral elements. *Trends in Plant Science* **10,** 586–593.

Witkowski ETF, Weiersbye-Witkowski IM, Przybylowicz WJ, Mesjasz-Przybylowicz J. 1997. Nuclear microprobe studies of elemental distributions in dormant seeds of *Burkea africana*. *Nuclear Instruments and Methods in Physics Research Section B: Beam Interaction with Materials and Atoms* **130,** 381–387.

Zhang C, Römheld V, Marschner H. 1995. Retranslocation of iron from primary leaves of bean plants grown under iron deficiency. *Journal of Plant Physiology* **146,** 268–272.

Zheng SJ, Yanf JL, He YF, Yu XG, Zhang L, You JF, Shen RF, Matsumoto H. 2005. Immobilization of aluminium with phosphorus in roots is associated with high aluminium resistance in buckwheat. *Plant Physiology* **138,** 297–303.